A THREE-DIMENSIONAL FINITE ELEMENT ANALYSIS OF THREE ROLL PLANETARY MILL

Shyue-Jian Wu, Yeong-Maw Hwang and Ming-Hu Chang

Department of Mechanical Engineering, National Sun Yat-sen University,

Kaohsiung, Taiwan 80424, Repulic of China

Keywords: three roll planetary rolling process, remeshing

ABSTRACT

The purpose of this paper is to analyze bar rolling process by means of three rolls planetary mill with a three-dimensional elastic-plastic finite element model. The problems can be solved with the aid of finite element program MARC by adopting the large deformation - large strain theory with the updated lagrangian formulation (ULF) and considering the contact problem between the rigid three rolls and the deformable bar billet. In addition, a remeshing procedure was adopted to improve the unexpected run time error of turning element inside out. Furthermore, a new subdivided element model of the divided layers was created, and two different kinds of deformable bar billet were used to simulate the process. The numerical results obtained, such as equivalent von-mises stress and plastic strain distribution, rolling force, rolling speed of the entrance and exit plane, etc, are very useful in designing the rolling process of three roll planetary mill.

INTRODUCTION

The three-roll planetary mill is a high-reduction machine with one pass, which is the most effective method for a high reduction rolling process than other conventional–type rolling process [1].

The mechanism of three-roll planetary mill is carried out in the following manner. The rolls are driven by a main drive planetary gear system and a superposed drive gear system

as shown in Fig.1. The superposed drive gear system will be driven additionally to eliminate any slight rotation of the outlet material. The axis of the roll can be adjusted to form an offset angle (α) and inclined angle (β), as shown in Fig.1 and Fig.2, respectively, the axes of three conical rolls are arranged at an angle of 120° in relation to one another, which rotate around the deformable bar billet. In general, the surface of rolls is composed of two parts, one is the reduction zone with a tapered cone, and the other is the smoothing zone with a smaller tapered cone and sphere fillet at the corner as shown in Fig.3. The round billets are conveyed through a supporting pipe located in the center of the three-roll mill by a back pushing rod unit, until it makes contact with the rolls in the pass and then rolled out. Various cross-sectional area of the product can be easily obtained by simply adjusting the axes of the three rolls. The three roll planetary mill is particular suited for making round billets. An important advantage of the three-roll mill is that during the process the operating temperature of the deformable bar billet is almost under an isothermal state.

A plasticine model mill simulated by means of rigid-plastic finite element method with the assumption of axis-symmetric model (approximately equivalent three dimensional model) of RPFEM by T. Noma, et al, [2]. Some useful results of three rolls planetary mill have been investigated by experiments with plasticine [3]. But it is very difficult to make a complete analysis for a whole simulation of the rolling process with a three dimensional element model. When a three-dimensional element model is used, it will take a large amount of computing time [4-6]. A model with 640 element and 1025 nodes having a steady state simulation will took 175 hours of CPU time on a vax-11/750,with about 2600 iteration [5]. This paper simplifies the analysis by ignoring the effect of the rotation of the sun gear during the rolling process. That is, the axis of the three roll rotates with its axis only as a rough prediction of these high reduction process of three-roll planetary mill.

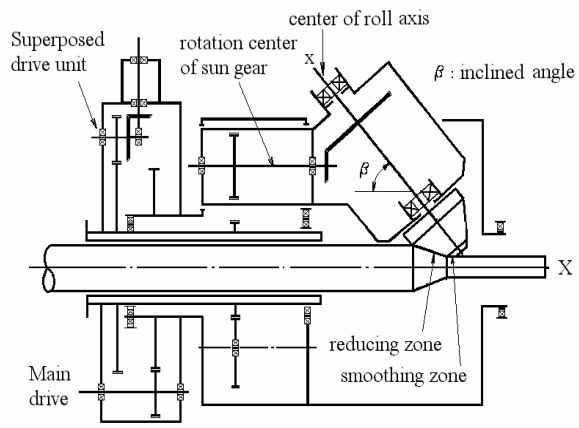

Fig.1. Schematic diagram of the three roll planetary mill

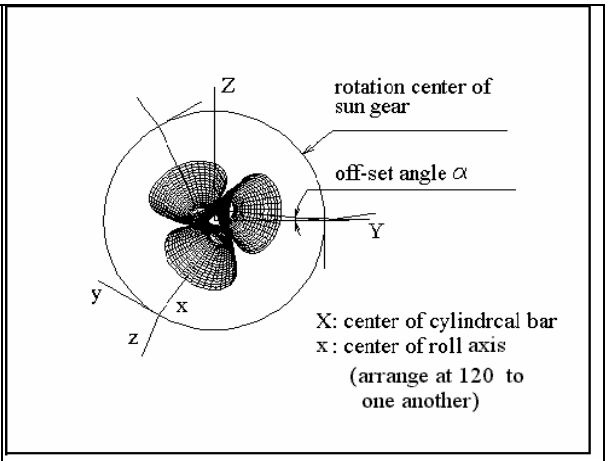

Fig.2. End view of the three roll planetary mill

The objective of this paper is to develop the mesh system inside the deformable bar billet and simulate the stress and strain distributions of the billet at the roll-gap by the finite element method with an elastic-plastic model. With a finite element package MARC [7-9], this research adopts a three-dimensional brick element model to simulate the three-roll planetary high reduction process. After numerical simulation, the bearing force of the roll, and the axial velocity of inlet and outlet in the steady state were calculated.

THE UPDATED LAGRANGE PROCEDURE

During metal forming process, the workpiece undergoes large plastic deformations and rotations. It is necessary to consider Geometric non-linearity, material non-linearity and constitutive non-linearity in the large strain plastic problem [10,11]. Based on the Truesdell rate of cauchy stress and the updated lagrangian formulation, a deformed continum can be described by a deformed configuration, and the rate of virtual work was derived as the following:

$$\int_v [\overset{\bullet}{\sigma}{}^{T}_{ij} \frac{\delta u_i}{\partial x_j} + \sigma_{ij} \frac{\partial v_k}{\partial x_i} \frac{\partial \delta u_k}{\partial x_j}] dv = \int_v \overset{\bullet}{q}_i \, \delta u_i dv + \int_s \overset{\bullet}{t}_i \delta_i ds \tag{1}$$

Where $\overset{\bullet}{\sigma}{}^{T}_{ij}$ is the Truesdell rate of cauchy stress, and u_i is the displacement field of the spatial particle, and x_i is the spatial position vector of a particle described as deformed coordinate configurations, and v_i is the velocity field of the spatial particle, and $\overset{\bullet}{q}_i$ is the rate of distributed load per unit volume in the deformed situation, and $\overset{\bullet}{t}_i$ is the rate of boundary (surface) load, the integration was carried out over the current volume and surface.

In this equation, the Truesdell rate of cauchy stress ($\overset{\bullet}{\sigma}{}^{T}_{ij}$) shows the close relationship with the usual rate of cauchy stress ($\overset{\bullet}{\sigma}_{ij}$) by:

$$\overset{\bullet}{\sigma}{}^{T}_{ij} = \overset{\bullet}{\sigma}_{ij} - \frac{\partial v_i}{\partial x_k} \sigma_{kj} - \sigma_{ik} \frac{\partial v_j}{\partial x_k} + \sigma_{ij} \frac{\partial v_k}{\partial x_k} \tag{2}$$

From [9] the constitutive equations for elastic-plastic materials is postulated in the form

$$\overset{\bullet}{\sigma}{}^{T}_{ij} = l_{ijkl} D_{kl} \tag{3}$$

where the deformation rate is defined by $D_{kl} = \frac{1}{2}\left(\frac{\partial v_k}{\partial x_l} + \frac{\partial v_l}{\partial x_k} \right)$, and the moduli l_{ijkl} is not equal to the classical elastic-plastic moduli L^{e-p}_{ijkl} the basis of the small-strain theory. The relation between the large strain moduli l_{ijkl} and the classical elastic-plastic moduli L^{e-p}_{ijkl} can be generalized as follows:

$$l_{ijkl} = L^{e-p}_{ijkl} - \delta_{il}\sigma_{kj} - \sigma_{ik}\delta_{jl} - \sigma_{ij}\delta_{kl} \tag{4}$$

However, the deformations are (near) incompressible, so the last term can be neglected and the constitutive equations remain symmetric.

*Treatment of contact

The initial contact position of the problem can be computed by the means of halving the interval (bisection method). In Fig.3, contact problem between the rigid body and deformable bar billet can be used as solver constraints in MARC [9]. The non-penetration constraint is defined by

$$\vec{u}_A \bullet \vec{n} \le D \tag{5}$$

Where $\vec{u}_A$ is the displacement vector of node A of the deformable bar billet, and $\vec{n}$ is the unit normal vector of rigid die, and D is the distance between the rigid die and deformable bar billet.

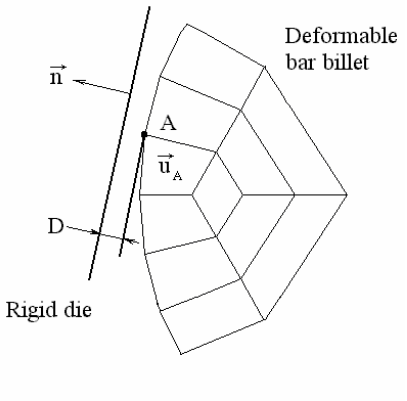

Fig.3 definition of contact problem

Whenever contact between a deformable body and a rigid body is detected, imposed displacement are automatically created. A check is made on all free boundary nodes to determine whether the newly calculated displacement increments put them inside any surface. If the increment is reduced, the current increment is considered split into two and the remainders are executed next.

* Treatment of friction

Friction has been traditionally modeled in the metal forming field in two ways: a coulomb type, and a constant shear type [9]. In this paper coulomb friction was used in the bar rolling process, which considers that there is a tangential force applied along an interface described by the equation:

$$\vec{f}_t \le -\mu f_n \vec{t} \tag{6}$$

where $\vec{f}_t$ is the tangential force being applied, and μ is the coefficient of friction, and

f_n is the normal reaction, and $\vec{t}$ is tangential unit vector in the direction of the velocity defined as follows:

$$\vec{t} = \frac{\vec{v}_r}{|\vec{v}_r|} \tag{7}$$

where $\vec{v}_r$ is the relative slide velocity of the contacted node.

Quite often in metal forming, neutral lines develop, which makes friction equation to an implicit step function of the displacement increment vector du.

A step function usually causes numerical problems. Therefore, a smoothing procedure is expected. The following one was made

$$\vec{f}_t = -\mu f_n \frac{2}{\pi} \tan^{-1}(\frac{|\vec{v}_r|}{C})\vec{t} \tag{8}$$

The constant C smoothen more or less the step function. Typically C should be one or two orders of magnitude lower than the average sliding velocity in the contact region. Equations automatically reproduce “sticking” region by allowing variable very small slip. It also avoids the logical steps of making the distinction between sticking and sliding.

* Treatment of remeshing

The element mesh of the deformable bar billet under the three-roll planetary rolling process, usually occurred a seriously distortion, even they might even cause elements turning inside out. To deal with this problem, a treatment of element mesh remeshing was adopted in this study [12]. To avoid the remeshed shape of outer circumferential of billet, it is necessary to highlight the effect of the scheme on the circumferential of the bar billet. In this paper, the remeshing increment was implemented once every 20 usual increments. The nodal points only in the interior of the bar billet showed a new position vector and other relative variables by averaging the position field variables.

RESULTS AND DISCUSSION

This research adopted two kinds of size of the billet to simulate the rolling processes, one is shown in Fig.4 for case A1 to A2, and the other is shown in Fig.5 for case A3 to A5. The numbering system of the bar billet of the elements and nodes are shown in Fig.6a, and Fig.6b. The material used in the analysis is stainless steel 316. It was assumed that the rolling process was conducted isothermally at 1100℃.The stress-strain relationship of stainless steel 316 at this temperature is obtained by compressing test and simply modeled by adopting a bilinear function . As shown in Fig.4 and Fig.5, the initial positions of the section No.1 for A1 to A5 are all the same.

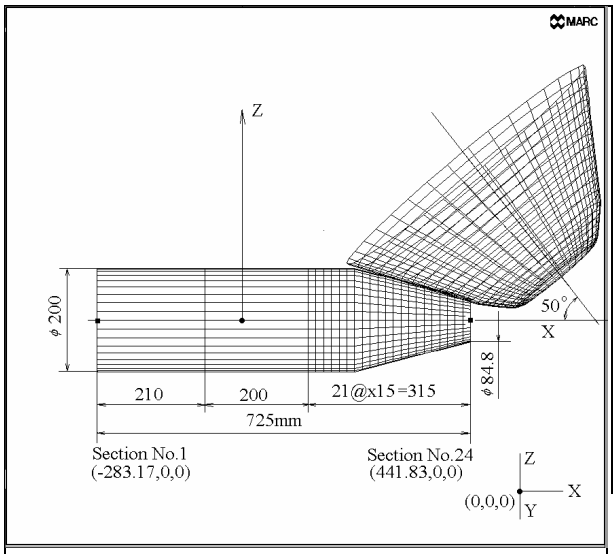

Fig.4. Deformable bar billet for case A1, A2

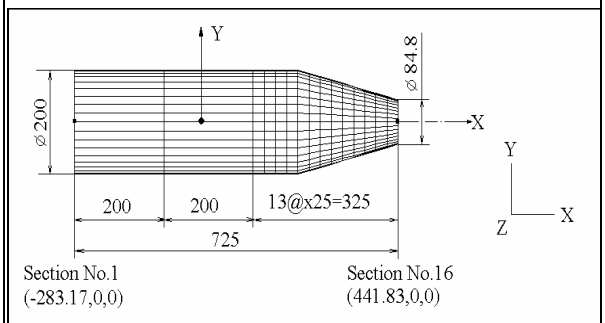

Fig.5. Deformable bar billet for case A3, A4, A5

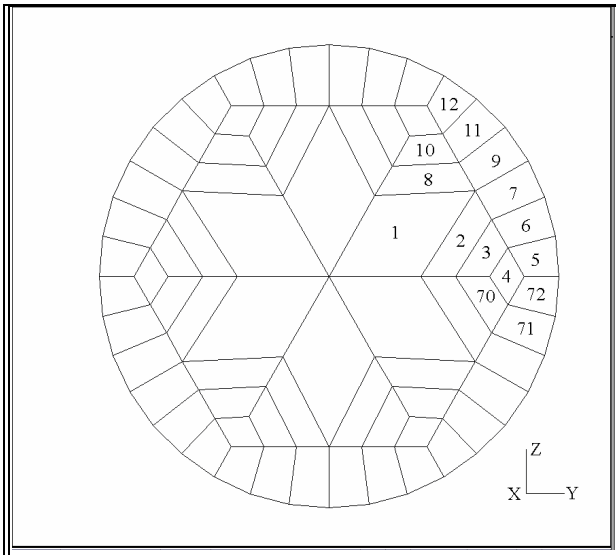

Fig.6a. Numbering system of elements

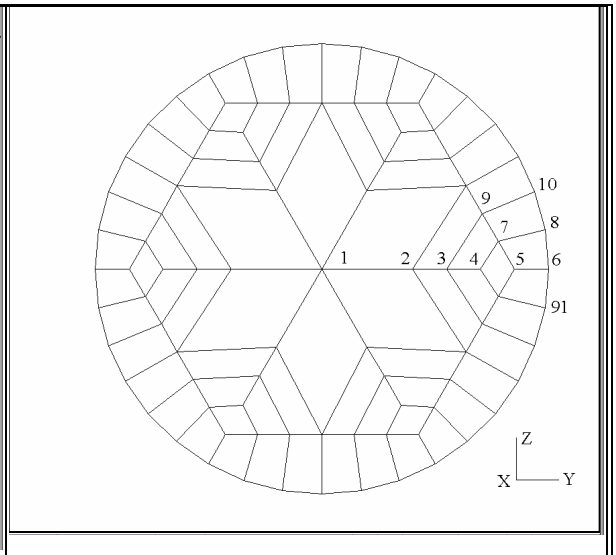

Fig.6b. Numbering system of nodes

The profile of the roll and initial contact configuration is shown in Fig.7, and Fig.8. The simulation of the three roll planetary is composed of a deformable bar billet, a back pushing plate to push the bar billet from left to right, a rigid supporting pipe to support the bar billet, and three rigid rolls to roll the deformable bar billet. Surface of rolls is used as a rigid body, on which are 20 divided along axial and 36 divided along circumferential of the cone of the roll.

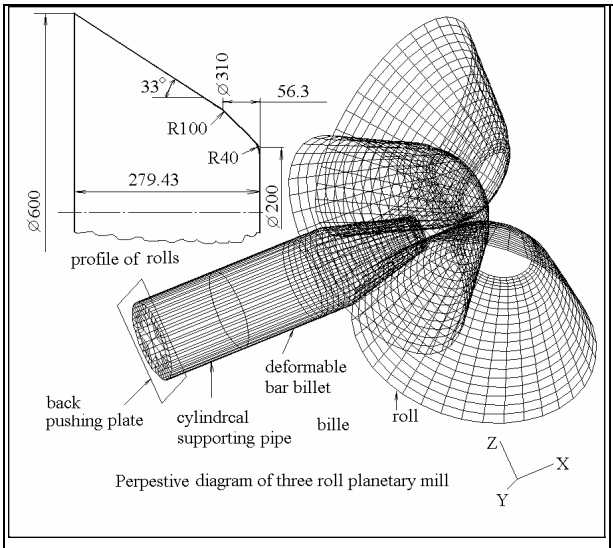

Fig.7. Initial contact condition and the profile of the roll

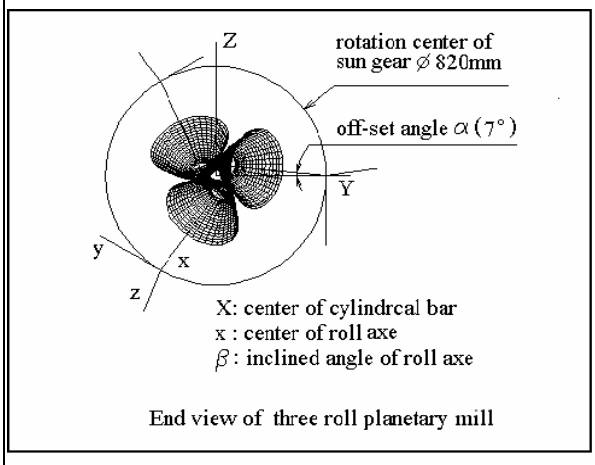

Fig.8. Configuration of three roll planetary mill

The material property are described in detail as follows:

Material: stainless steel 316 under circumference of 1100℃

Strain hardening rate (H): 116MPa (ε <0.50) and 10MPa ($\varepsilon \geqq 0.50$)

Young's modulus (E): 79MPa

Yielding stress: 100MPa

Poisson's ratio: 0.33

Coefficient of friction between the roll and the deformable bar billet: 0.5 ~ 0.7

Inclined angle (b): 50°

Offset angle (a): 7°

Every three-dimensional brick element bears a total 24 degrees of freedom and with three degrees of freedom per node. The element properties of the deformable bar billet for simulation in this study was tabulated as follows:

Table.1. The detailed description of the simulated case A1~A5

<table>
<tr><th></th><th>Element property</th><th>Angular velocity of the roll</th><th>Axial increment of Back pushing plate</th><th>Axial increment of supporting pipe</th><th>Coefficient of friction</th></tr>
<tr><td>A1</td><td rowspan="4">Node=2184
Element =1656
Layer=23
Section=24</td><td rowspan="5">0.01rad/unit time step, with one remeshing increment after every each 20 unit time step increment</td><td rowspan="5">1.0mm/unit time step only for initial state to increment No.20</td><td rowspan="5">Departed from the section No.1 after 20's unit time step increment</td><td>0.5</td></tr>
<tr><td>A2</td><td>0.6</td></tr>
<tr><td>A3</td><td rowspan="3">Node=1456
Element =1080
Layer=15
Section=16</td><td>0.5</td></tr>
<tr><td>A4</td><td>0.6</td></tr>
<tr><td>A5</td><td>0.7</td></tr>
</table>

In the present study, it was necessary to push the deformable bar billet to the stage as shown in Fig.7. When the friction force was large enough, the roll will pull the deformable bar billet in. For the firstly initial 20 unit time increments, the back pushing velocity is

simulated by setting (1.0mm/unit time increment), and the angular velocity of roll was rotated by setting (0.01rad/unit time increment), and the supporting pipe will depart from the leftmost section at the end of increment No. 20, after that the process is simulated merely by rotating the rolls only.

From the simulated results, it is shown in Fig.9, the pushing plate is no longer contacting the end of the deformable bar billet at increment No.175 for case A1. The force of back pushing plate from an initial state to an increment 250 for each case A1 to A5 is shown in Fig.10. Accordingly, one can realize that the case A5 has a high value of force of 3.0E+06 N with a higher friction coefficient 0.7, and the plate departed from the leftmost section faster than other case also. Generally, it is the coefficient of friction plays an important roles, the billet will leave faster from the back pushing plate as the friction is larger.

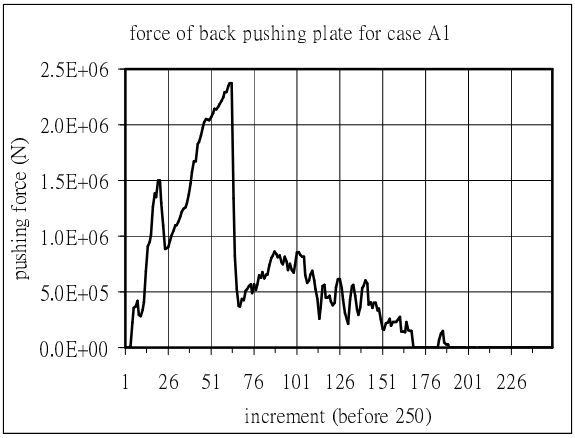

Fig.9. The rolling force of case A1

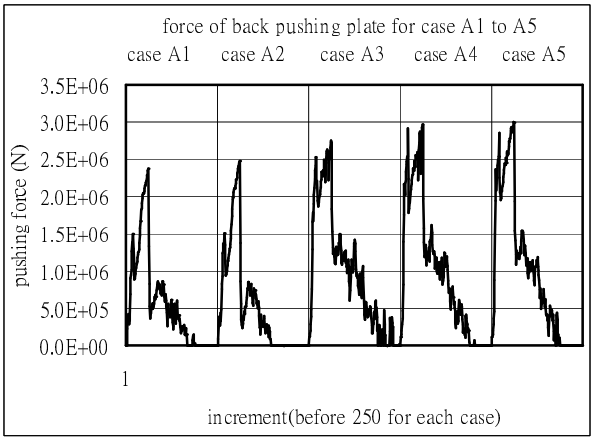

Fig.10. The rolling force of case A1~A5

Grid distortion of the front views from unit time increment No.100 to 800 of the deformable bar billet are shown in Fig 11~18. It is found that in the case A1 the equivalent von-mises stress and plastic strain at increment No.700 are 237MPa and 9.062. When the layer No.12 of case A2 is rolled out, the computed equivalent von-mises stress and plastic strain of the bar illustrated in Fig.19 and Fig.20, reach to 309MPa and 15.61, respectively. In

fact, the deformable bar billet undergoes an area reduction more than 700% as the original diameter of the bar is 200mm and final reduced diameter is 75mm.

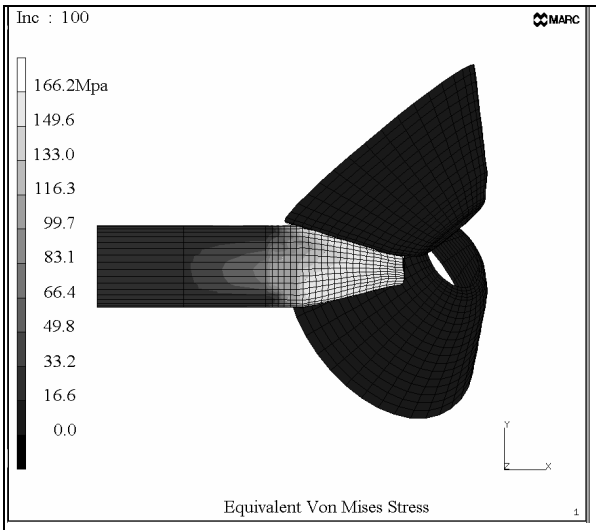

Fig.11. The equivalent von mises stress for case A1

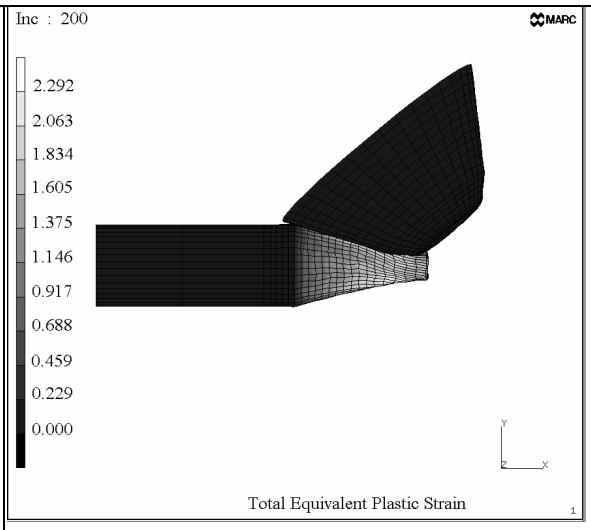

Fig.12. The Equivalent plastic strain for case A1

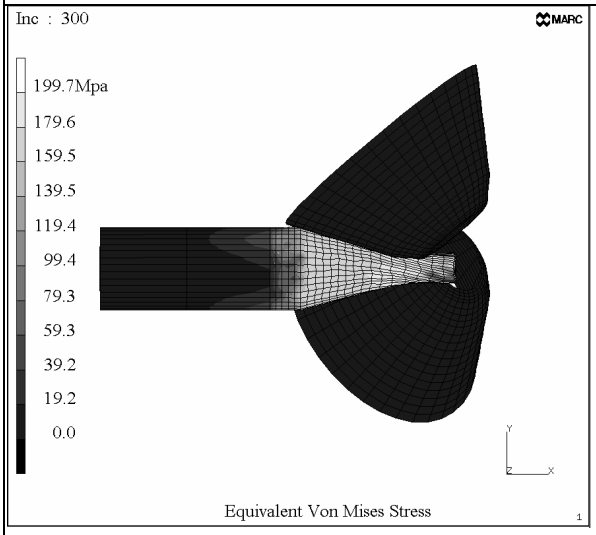

Fig.13 The equivalent von mises stress for case A1.

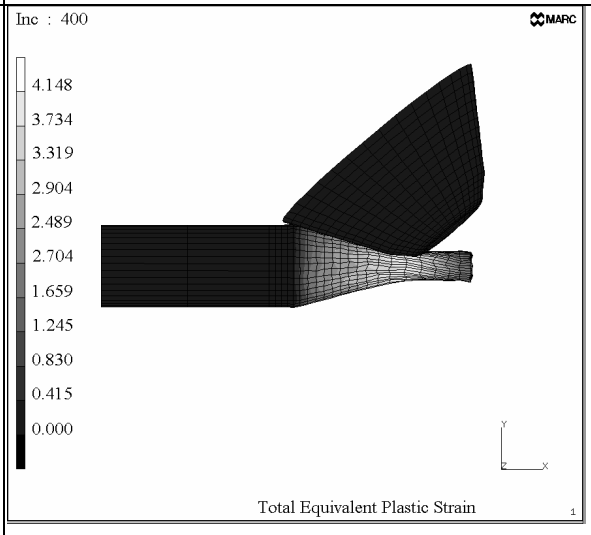

Fig.14. The Equivalent plastic strain for case A1

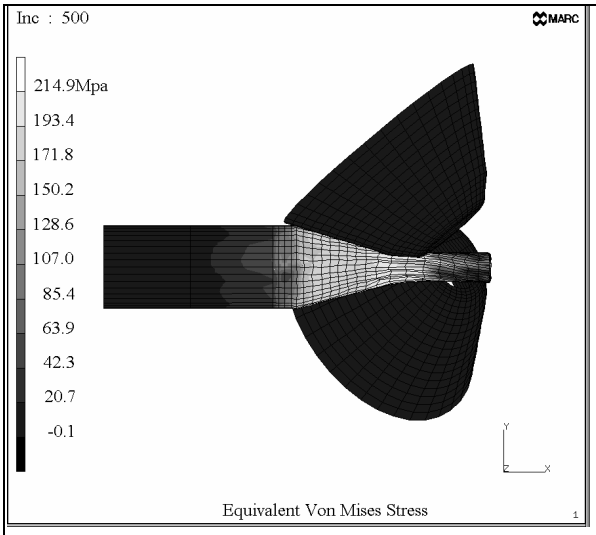

Fig.15. The equivalent von mises stress for case A1

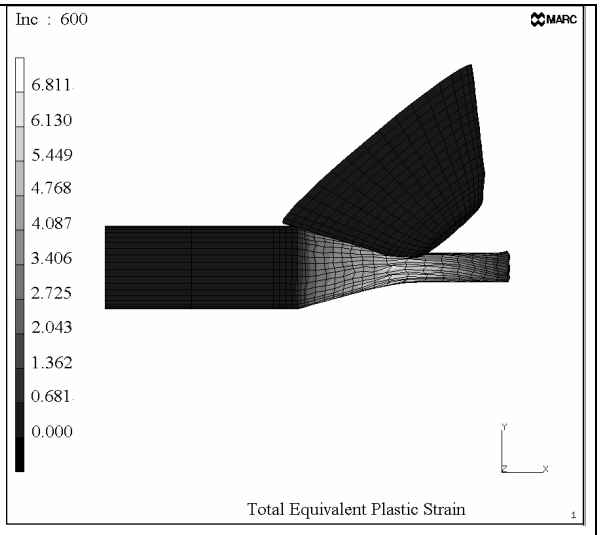

Fig.16. The Equivalent plastic strain for case A1

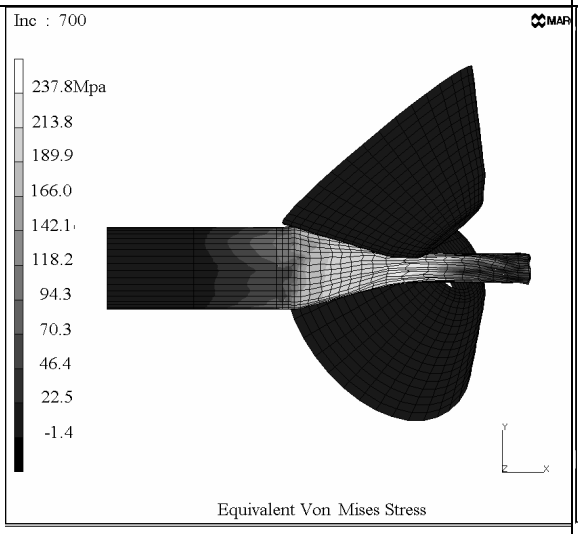

Fig.17. The equivalent von mises stress for case A1

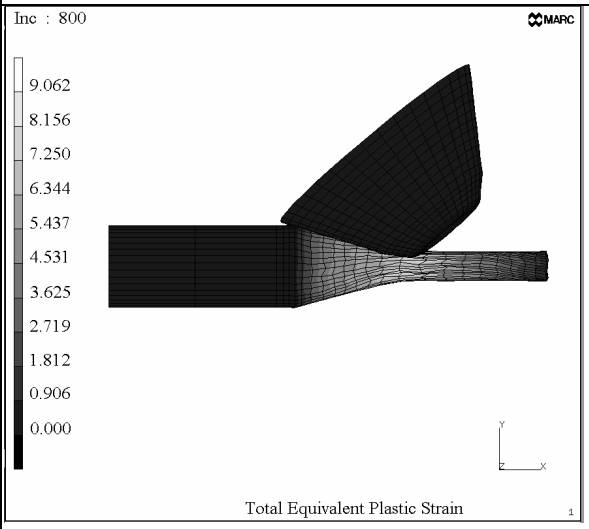

Fig.18. The Equivalent plastic strain for case A1

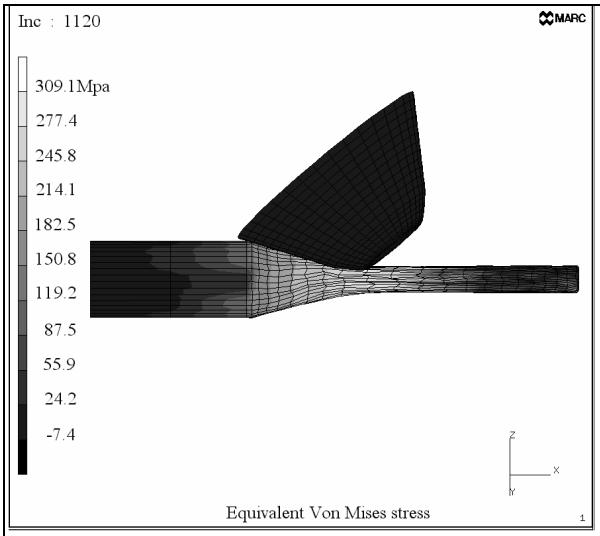

Fig.19. The equivalent von mises stress for case A2

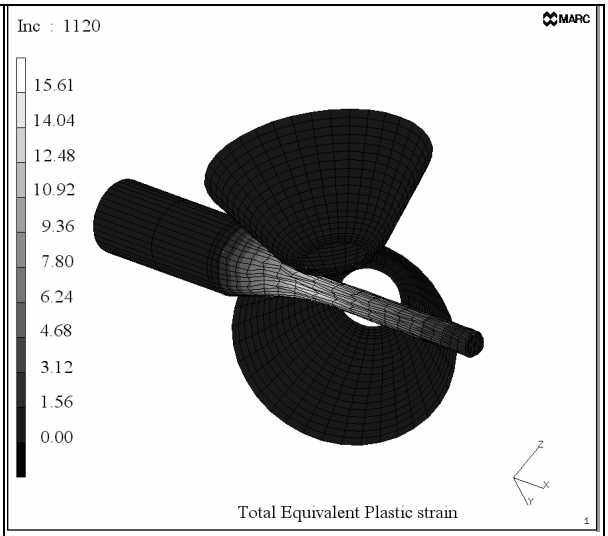

Fig.20. The Equivalent plastic strain for case A2

It can be easily determined by checking that the fluctuated bearing force of roll is circulating between increment No.400 and No.700 (Fig.21). It seems that the deformation reached steady state at unit time increment between 400 to 700 (Fig.22), and that it becomes non-steady beyond the increment 850 because the inlet element mesh is very large and still in an elastic state. Note that the rolling force fluctuated in the process because some of the circumferential nodes are contacted with and/or departed from the rolls. The bearing force components of Y and Z direction mean the reduction force required to reduce the section area, and X direction stand for the velocity of deformable bar billet driven by the rolls. The total and component of historic bearing force of roll for case A2 and A3 are shown in Fig.23, Fig.24, and Fig.25, and Fig.26, respectively. Table.2 listed the fluctuated force of rolls at steady state for cases A1 to A3.

Table.2. Comparison of the fluctuated force of roll at steady state for case A1 to A3

Case	Increment	F (KN)	Fx (KN)	Fy (KN)	Fz (KN)
A1(μ =0.50)	400~700	2300~2650	150~220	2100~2400	800~1000
A2(μ =0.60)	400~700	2450~2900	200~300	2300~2700	1000~1200
A3(μ =0.50)	400~700	2600~3150	200~300	2400~2990	1000~1280

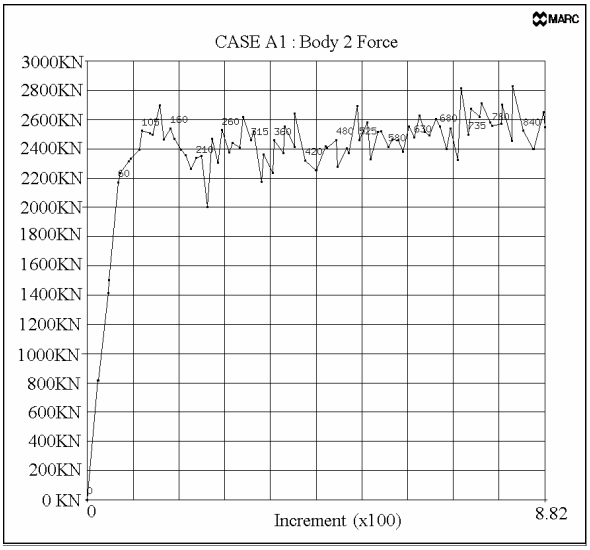

Fig.21. The bearing force of roll

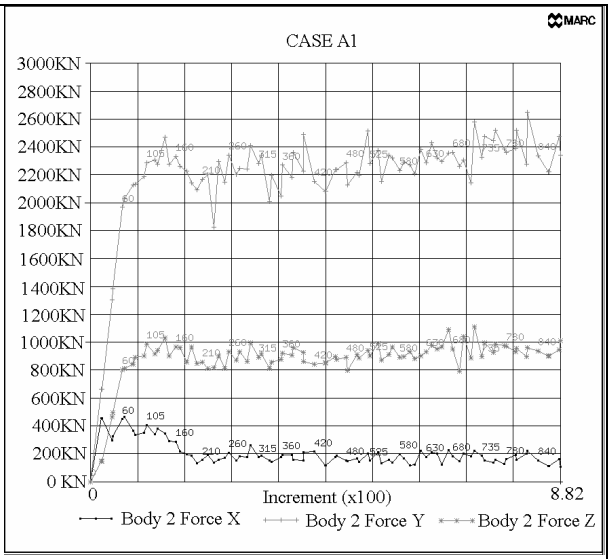

Fig.22.The bearing force components of roll

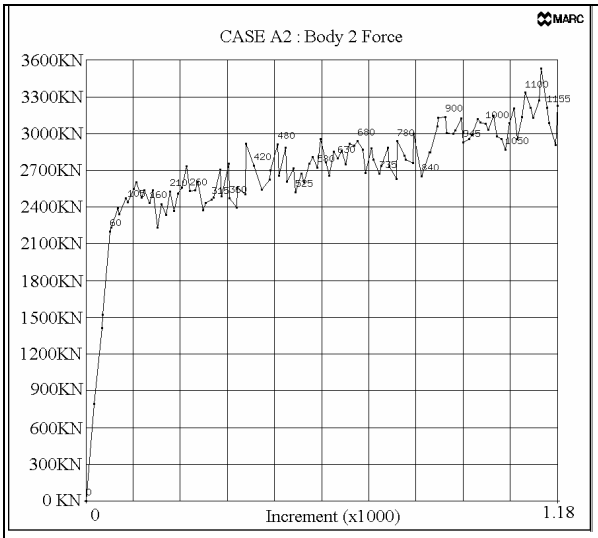

Fig.23. The bearing force of roll

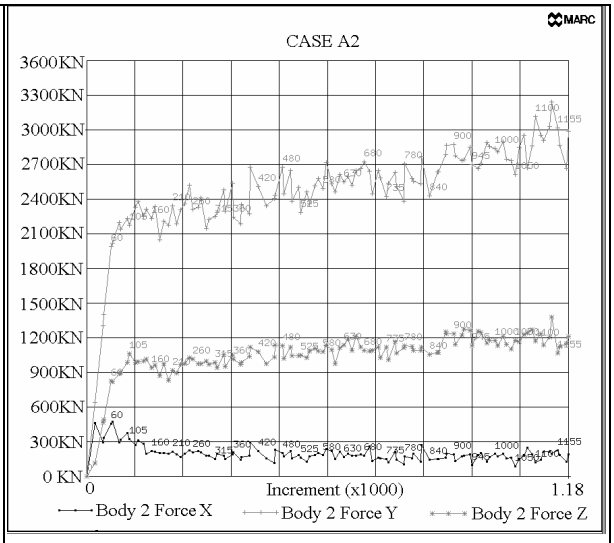

Fig.24. The bearing force components of roll

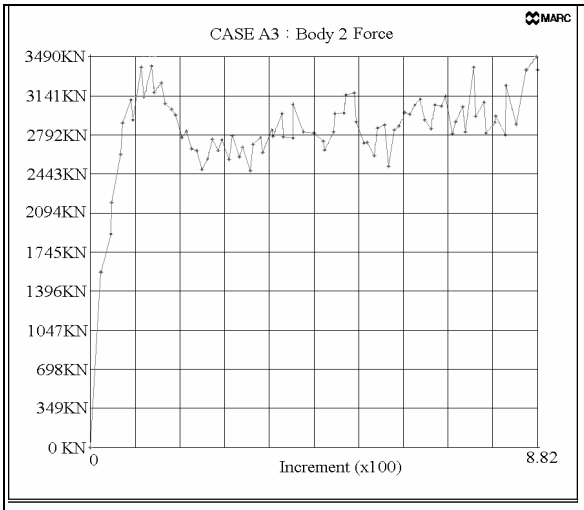

Fig.25. The bearing force of roll

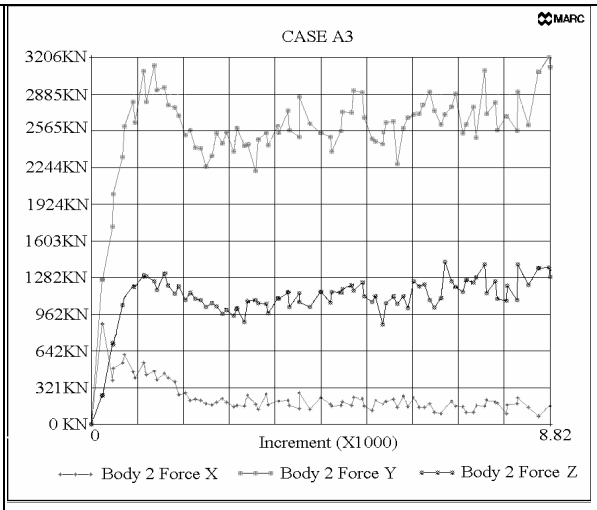

Fig.26. The bearing force components of roll

Figure 27 demonstrated the axial velocity of nodal point at inlet and outlet along global coordinates. When a steady state occurred, the axial velocities of the inlet and outlet are 0.09mm and 0.53mm per unit time, and its ratio is converging to 6.0 approximately, as shown in Fig.28. The average mean diameter of the circumferential nodes on each section from initial state to unit time increment No.800 is shown in Fig.29. When the figure was partly enlarged as shown in Fig.30, it can be seen the bulge effects on the inlet near the deformation zone, in other words the bulge amount are large at increment No.200 to 400 than that at increment No.600 to 800.

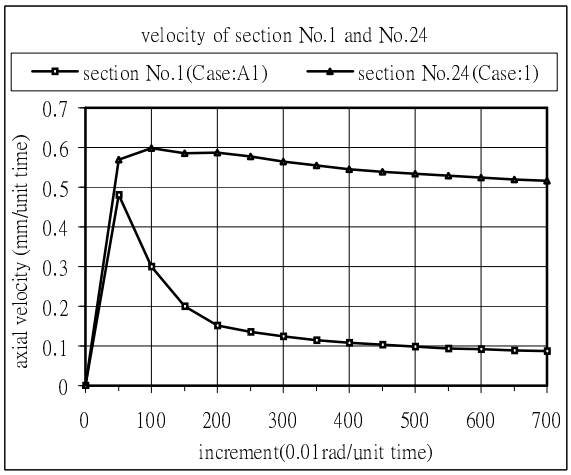

Fig.27. The axial velocity of the inlet and outlet

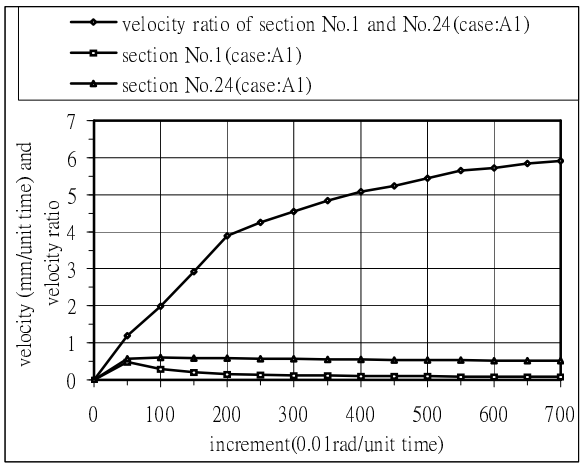

Fig.28. The velocity ratio of inlet and outlet

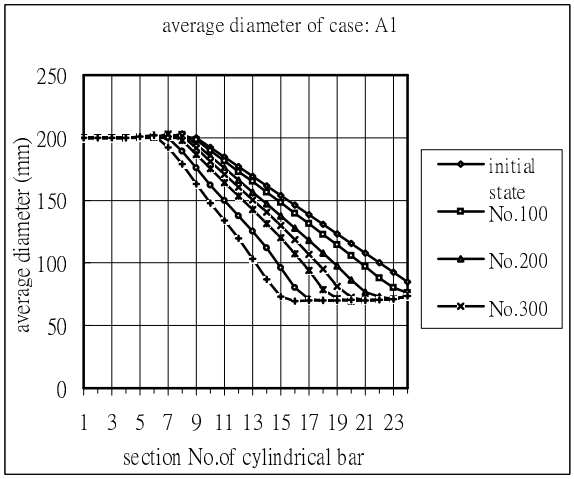

Fig.29. The average mean diameter of each section

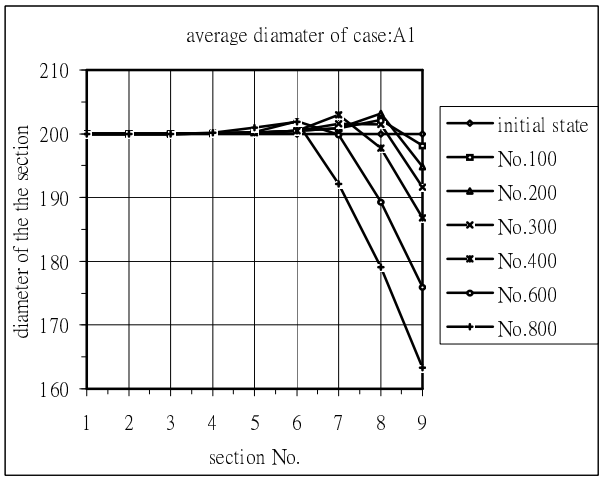

Fig.30. The enlarged diagram of left part of Fig.29

Fig. 31 illustrates the axial nodal position of rightmost section of case A1 to A5. And Fig 32 shows the axial nodal velocity of rightmost section of case A1 to A5. In shorts, the greater the friction value is, the larger the velocity produced is.

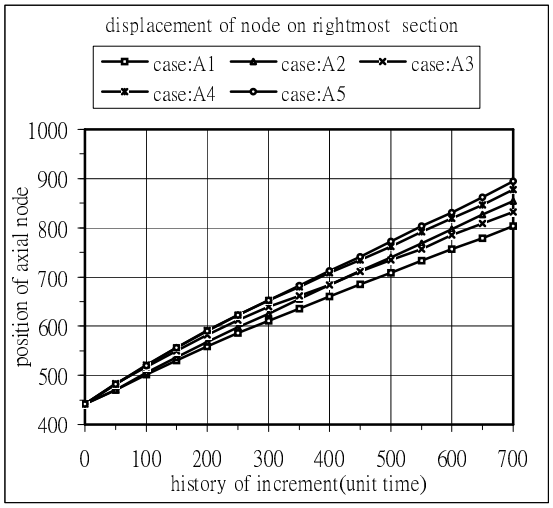

Fig.31.The axial position of axial node on rightmost section.

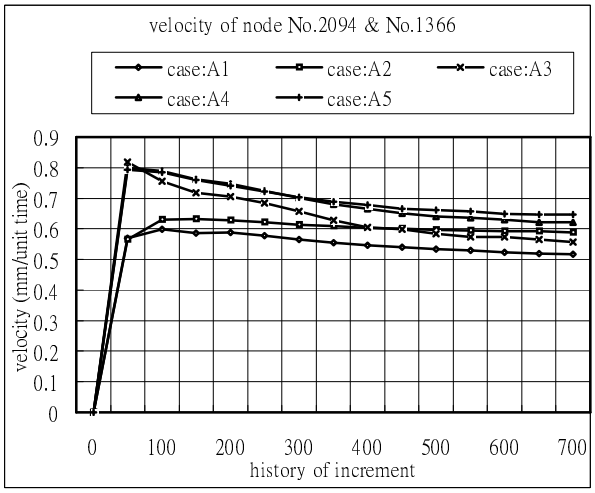

Fig.32. Comparison of the velocity of axial node on rightmost section.

CONCLUSION

This research proved the possibility of the new subdivided element for the simulation of three roll planetary rolling process, it is also suggested that the circumferential nodal point and the section element subdivided should posses a symmetrical relation with the numbers of roll. With the amounts of deformation occurring in the process, the remesh scheme should be added for further implementing. The total computation required on a CONVEX C3840 for each case A1~A2 and A3~A5 are about 5000 and 3000 CPU minutes, respectively. For the sake of saving computing time, from the simulated results, a smaller degree of freedom of problem should be adopted. In the present analysis the rolls are rotated with its axe only, but the simulated stress and strain distribution, bearing force of rolls, velocity ratio of the inlet and outlet are good for the rough predict of the first time.

REFERENCES

1. W. Jurgen Ammerling, et al., ”The knocks 3-roll technology for high precision specialty rod and bar products”, MPT-Metallurgical Plant and Technology, Vol.6, pp14-19, 1989
2. T. Noma, T. Tsuta, and K. Kadota, “ Three-roll planetary mill developed and installed

first in Japan", steel plant & machinery department, KHI, Ltd/Japan, session 1B/2-0~1B/2-17

3. Koushiro Aoyagi and Kuniteru Ohta," Material deformation, rolling load and torque in 3-roll planetary mill", J. Japan, Society for Technology of Plasticity, Vol 24, pp.1039-11047, 1983-10
4. Guo-Ji Li and S Kobayashi, "Rigid plastic finite-element analysis of plane strain rolling", J. Engng. Indust. Vol 104, pp.55-64, 1982
5. J. J. Park, and S. I. Oh, "Application of three dimensional Finite Element analysis to shape rolling processes", J. Engng. Indust, Vol 112, pp.36-46, 1990
6. K. Mori and K. Osakada, "Finite element simulation of three-dimensional deformation in shape rolling", Int. J. Numer. Methods Engng, Vol 30, pp.1431-1440, 1990
7. J. C. Nagtegaal and J. E. DE Jong, "some computational aspects of elastic-plastic large strain analysis", Int. J. Numer. Methods. Engng, Vol 17, pp.15-41, 1981
8. I. Pillinger, P. Hartley, C. E. N. Sturgess and G .W. Rowe, "Use of a mean-normal technique for efficient and numerically stable large-strain elastic finite element solutions", Int. J. Mech. Sci. Vol. 28. No.1, pp23-29, 1986
9. Ir a.W.a. Knoter, "Special topic course on metal forming analysis using the finite element methods", Zoetermeer, October 15 and 16 1987. MARC Analysis Research corporation-Europe
10. R. M. McMeeking and J. R. Rice, " Finite-element formulations for problems of large elastic-plastic deformation", Int. J. Solids structures, Vol 11,pp601-616, 1975
11. H. D. Hibbitt, P. V. Marcal and J. R. Rice, "A finite element formulation for problems of large strain and large displacement", Int. J. Solids structures, Vol. 6, pp.1069-1086, 1970
12. J. H. Yoon and D. Y. Yang, "A three-dimensional rigid-plastic finite element analysis of bevel gear forging by using a remeshing technique", Int. J. Mech. Sci. Vol.32 No.4, pp.277-291, 1990